Supplement of Biogeosciences, 14, 5189–5216, 2017
https://doi.org/10.5194/bg-14-5189-2017-supplement

Biogeosciences Open Access EGU

Supplement of

Year-round CH_4 and CO_2 flux dynamics in two contrasting freshwater ecosystems of the subarctic

Mathilde Jammet et al.

Correspondence to: Mathilde Jammet (mathilde.jammet@ign.ku.dk)

Contents:

Text S1: Development of the gap filling models using artificial neural networks

Gap filling of the CH_4 flux time series was performed separately on the lake and fen flux datasets, using artificial neural networks (ANN) (Dengel et al., 2013; Moffat et al., 2010; Papale and Valentini, 2003). Artificial neural networks (ANNs) are multivariate, non-linear regression models (Bishop 1995) that are fully empirical: the observational data are used to constrain the model's numerical relationship between the inputs (independent variables) and output (dependent variable) (Papale and Valentini 2003, Moffat et al 2010).

An artificial neural network is composed of nodes that are organized in layers and inter-connected. Each connection carries a weight that is analogous to a nonlinear regression parameter (Moffat et al., 2010). The development of the model consists of a training phase, followed by a testing (validation) phase. The weights are assigned and modified during the training phase, until reaching an optimal value. The network is trained by receiving sets of input data (independent variables i.e. environmental drivers) and associated output data (dependent variables i.e. flux time series). The training dataset was built by randomly selecting 40% of the available data pairs (environmental variables and associated flux data) and the testing set was selected as a randomly picked 40 % of the remaining available data pairs. The subsets were selected so that each season was represented.

Environmental variables to be included as inputs were selected according to their physiological relevance to the production of CH_4 and their transport from the surface to the atmosphere, as reported in the literature. These included peat temperature (for the wetland), surface sediment temperature and water temperature (for the lake), air temperature, wind speed, air pressure, net radiation at the surface and incoming solar radiation (for both). The relevance of the drivers was confirmed by correlation analysis. Before being used as input to the ANNs, the environmental variables have to be gap-free. On the period of interest, 10 to 25 % of the environmental input data was missing. These were filled using the online tool developed by Reichstein et al (2005) available at http://www.bgc-jena.mpg.de. Additional "fuzzy" datasets can be introduced as input variables to "force" a temporal parameter onto the modeled flux data, as described in Papale and Valentini (2003). Four fuzzy sets were used in this study, representing summer, autumn, winter and spring, respectively. The use of these fuzzy sets increased the performance of the ANNs to predict observed values, as seen by increasing r^2.

The networks comprised one input layer, one hidden layer where the neurons (nodes) receive the input values, each with an assigned weight, and one output layer. The addition of a hidden layer did

not improve the performance of the network. The number of neurons to include in the hidden layer was chosen by running the ANNs with 5 to 12 neurons, and choosing the number of neurons low enough to keep the model simple yet high enough to minimize the error of the model and maximize the correlation coefficient. Eventually, 6 neurons for fen CH_4 fluxes and 9 neurons for lake CH_4 fluxes were chosen.

The networks were developed on the hourly scale to reduce uncertainty by reducing the proportion of missing values. All variables were scaled between 0 and 1 before training (Papale and Valentini 2003) in order to remove potential bias due to the different numerical scale of the variables, and because a sigmoid function was used as transfer function between the neurons and the output values. At the end of the procedure the output variable is rescaled to their original units. The networks were optimized using the back-propagation algorithm (Dengel et al., 2013; Moffat et al., 2007; Papale and Valentini, 2003). For each set (lake and fen), the runs were repeated; the best runs - with the highest r^2 in the training phase between observed and modeled - were chosen and averaged as the main output. The gaps in the measured CH_4 flux time series were replaced by predicted values, and the annual sum was computed by integrating the hourly flux values over time.

The CO_2 flux data from the fen were gap filled in the same way by developing an ANN on the fen flux dataset. Input variables were photosynthetic active radiation (PAR), air temperature, vapour pressure deficit (VPD) and net radiation at the fen surface. Net radiation showed to be relevant for night time data. Furthermore, previously mentioned fuzzy sets were incorporated too. The final selected network was built with 6 neurons.

References

Dengel, S., Zona, D., Sachs, T., Aurela, M., Jammet, M., Parmentier, F. J. W., Oechel, W. and Vesala, T.: Testing the applicability of neural networks as a gap-filling method using CH4 flux data from high latitude wetlands, Biogeosciences, 10(12), 8185–8200, doi:10.5194/bg-10-8185-2013, 2013.

Moffat, A. M., Papale, D., Reichstein, M., Hollinger, D. Y., Richardson, A. D., Barr, A. G., Beckstein, C., Braswell, B. H., Churkina, G., Desai, A. R., Falge, E., Gove, J. H., Heimann, M., Hui, D., Jarvis, A. J., Kattge, J., Noormets, A. and Stauch, V. J.: Comprehensive comparison of gap-filling techniques for eddy covariance net carbon fluxes, Agric. For. Meteorol., 147(3–4), 209–232, doi:10.1016/j.agrformet.2007.08.011, 2007.

Moffat, A. M., Beckstein, C., Churkina, G., Mund, M. and Heimann, M.: Characterization of ecosystem responses to climatic controls using artificial neural networks, Glob. Change Biol., 16(10), 2737–2749, doi:10.1111/j.1365-2486.2010.02171.x, 2010.

Papale, D. and Valentini, R.: A new assessment of European forests carbon exchanges by eddy fluxes and artificial neural network spatialization, Glob. Change Biol., 9(4), 525–535, doi:10.1046/j.1365-2486.2003.00609.x, 2003.

Reichstein, M., Falge, E., Baldocchi, D., Papale, D., Aubinet, M., Berbigier, P., Bernhofer, C., Buchmann, N., Gilmanov, T., Granier, A., Grünwald, T., Havránková, K., Ilvesniemi, H., Janous, D., Knohl, A., Laurila, T., Lohila, A., Loustau, D., Matteucci, G., Meyers, T., Miglietta, F., Ourcival, J.-M., Pumpanen, J., Rambal, S., Rotenberg, E., Sanz, M., Tenhunen, J., Seufert, G., Vaccari, F., Vesala, T., Yakir, D. and Valentini, R.: On the Separation of Net Ecosystem Exchange into Assimilation and Ecosystem Respiration: Review and Improved Algorithm, ResearchGate, 11(9), 1424–1439, doi:10.1111/j.1365-2486.2005.001002.x, 2005.

Text S2: Pre-processing of raw CH_4 data

During the period of faulty electronic transmission of CH_4 measurements to the data logger (August 2013 to December 2014), CH_4 raw data from the FGGA were synchronized with the high frequency data logged onto the CR3000. Raw data stored on the FGGA memory are not sampled at exactly 10 Hz but at a variable frequency (11 to 12 Hz). Raw CH_4 data were thus linearly interpolated on 10 Hz timestamps to match the clock from the data logger. Additionally, to prevent mistakes due to a potentially uncalibrated clock on the FGGA, we did not use only the timestamp to synchronize the dataset. It was done in half-hour moving chunks of data by maximizing the correlation between logger data and FGGA data. The time showing the best correlation was chosen as a reference to adjust the clock, then CH_4 data were linearly interpolated onto the correct timestamp. Thus, when computing fluxes over this period, the time lag for CH_4 fluxes was set to be searched within a large window spanning that included 0s. After flux calculation, half-hours for which the synchronization procedure could not yield any reliable flux (i.e. where the method failed) were identified (lack of significant peak in the cross-covariance function, as in (Nordbo et al., 2012; Rinne et al., 2007; Wienhold et al., 1994)) and filtered out. This screening step was considered as a quality check of the synchronization procedure.

References

Nordbo, A., Järvi, L. and Vesala, T.: Revised eddy covariance flux calculation methodologies – effect on urban energy balance, Tellus B, 64(1), 18184, doi:10.3402/tellusb.v64i0.18184, 2012.

Rinne, J., Taipale, R., Markkanen, T., Ruuskanen, T. M., Hellén, H., Kajos, M. K., Vesala, T. and Kulmala, M.: Hydrocarbon fluxes above a Scots pine forest canopy: measurements and modeling, Atmospheric Chem. Phys., 7(1), 3361–3372, doi:10.5194/acp-7-3361-2007, 2007.

Wienhold, F. G., Frahm, H. and Harris, G. W.: Measurements of N2O fluxes from fertilized grassland using a fast response tunable diode laser spectrometer, J. Geophys. Res., 99(D8), 16557–16567, doi:10.1029/93JD03279, 1994.

Table S1: Total (fen + lake) flux data coverage after post-processing, for each season and year, in numbers of half-hourly values per period. Corresponding relative coverage in % is in parenthesis.

	Ice-free 1	**Ice-free 2**	**Ice-free 3**	**Ice-cover 1**	**Ice-cover 2**	**Ice-out 1**	**Ice-out 2**	**Year 1**	**Year 2**
CH_4	2376 (0.35)	4009 (0.58)	1731 (0.28)	1955 (0.22)	687 (0.08)	1616 (0.82)	979 (0.39)	5947 (0.34)	5468 (0.31)
CO_2	2240 (0.34)	1257 (0.18)	2599 (0.42)	2157 (0.25)	1249 (0.15)	1080 (0.55)	950 (0.38)	5619 (0.32)	3282 (0.19)

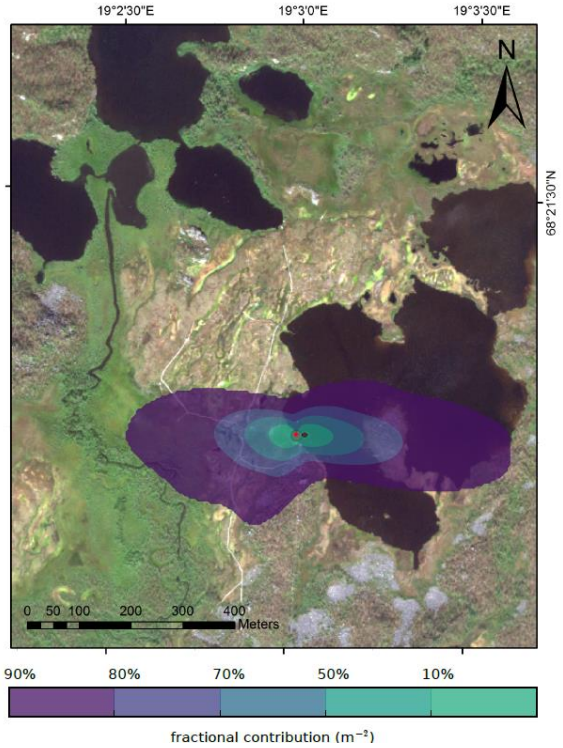

Figure S1. Flux footprint of the flux tower in winter averaged over all years. The location of the flux tower is indicated as a red circle.

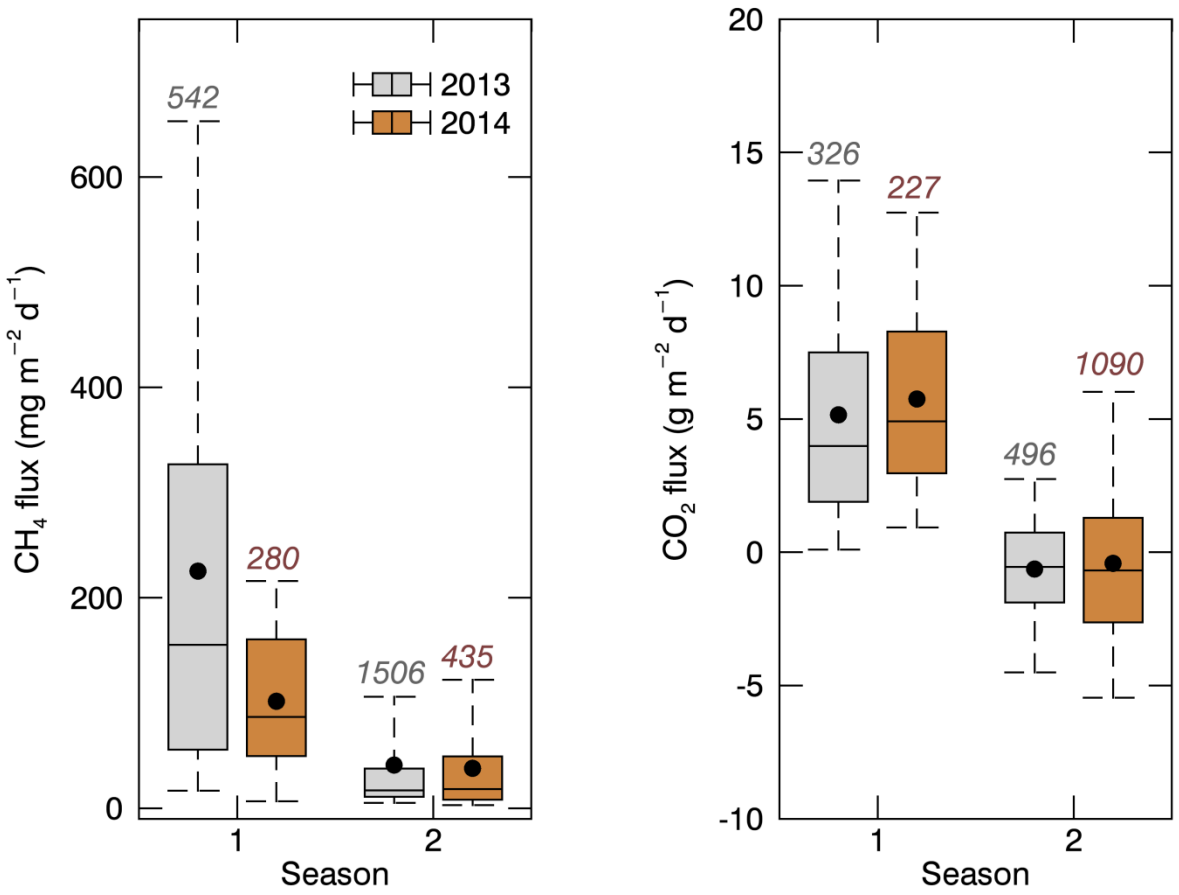

Figure S2. Significance of the CH_4 (left panel) and CO_2 (right panel) degassing rates at the lake during lake overturn (Season 1), as compared to flux rates during the following ice-free season (Season 2), in 2013 (grey boxes) and 2014 (brown boxes). The central line of the boxplots shows the median, box edges show 25th and 75th percentiles, and whiskers show 5th and 95th percentiles. The black dots indicate the mean flux rate. Outliers are not displayed. Only the main degassing peak, rather than the entire thaw season, was used to draw the figure. Numbers in italic indicate the amount of data available for each period.

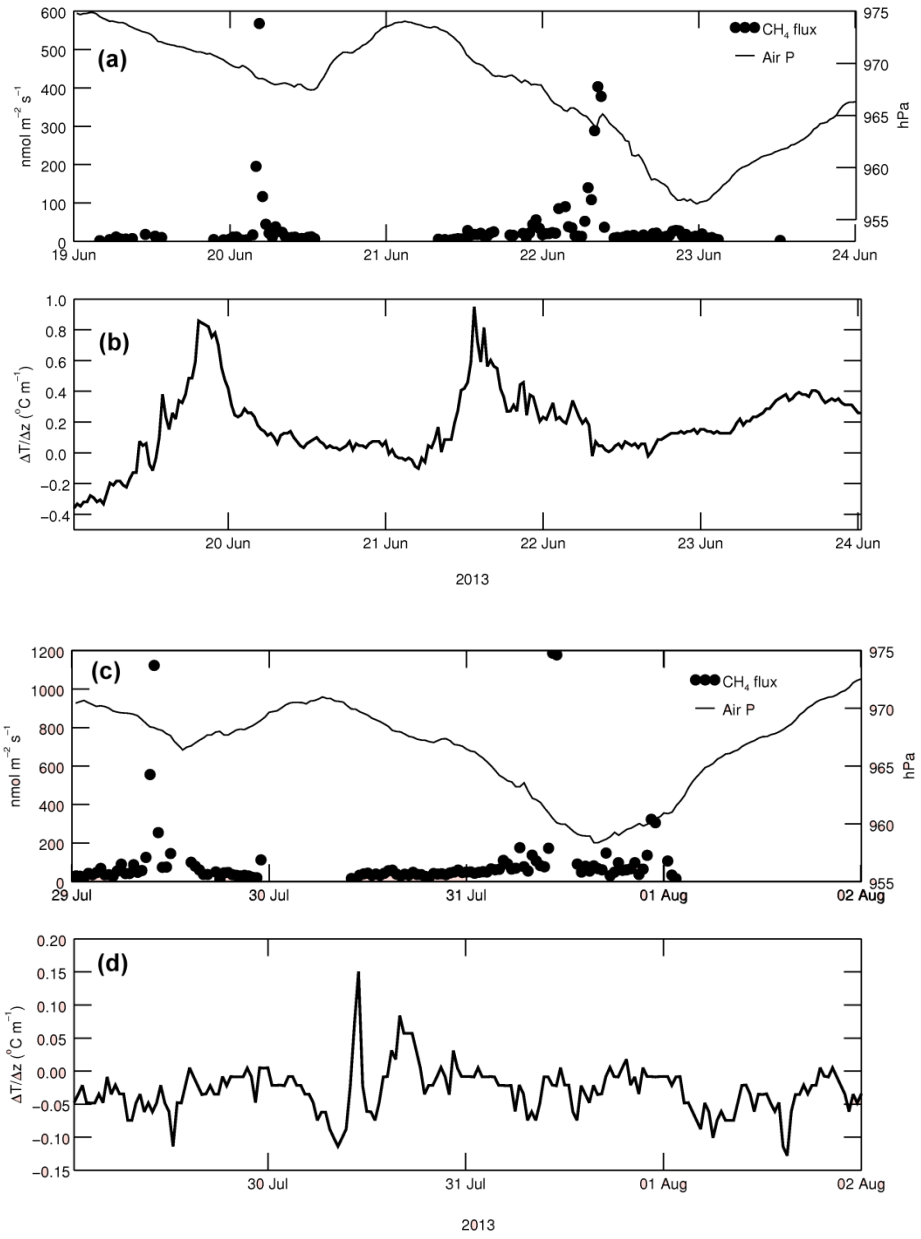

Figure S3. At the lake: example of periods during the summer when breakdown of a small thermal gradient (0.8-1.0 ˚C) between top (10 cm) and bottom (1 m) of the water column during morning hours (b) was coincident with CH_4 degassing and decreasing atmospheric pressure at the lake (a), which can indicate the effect of water-side convection; while most degassing events occurred at decreasing air pressure but nearly-isothermal water column (c-d).

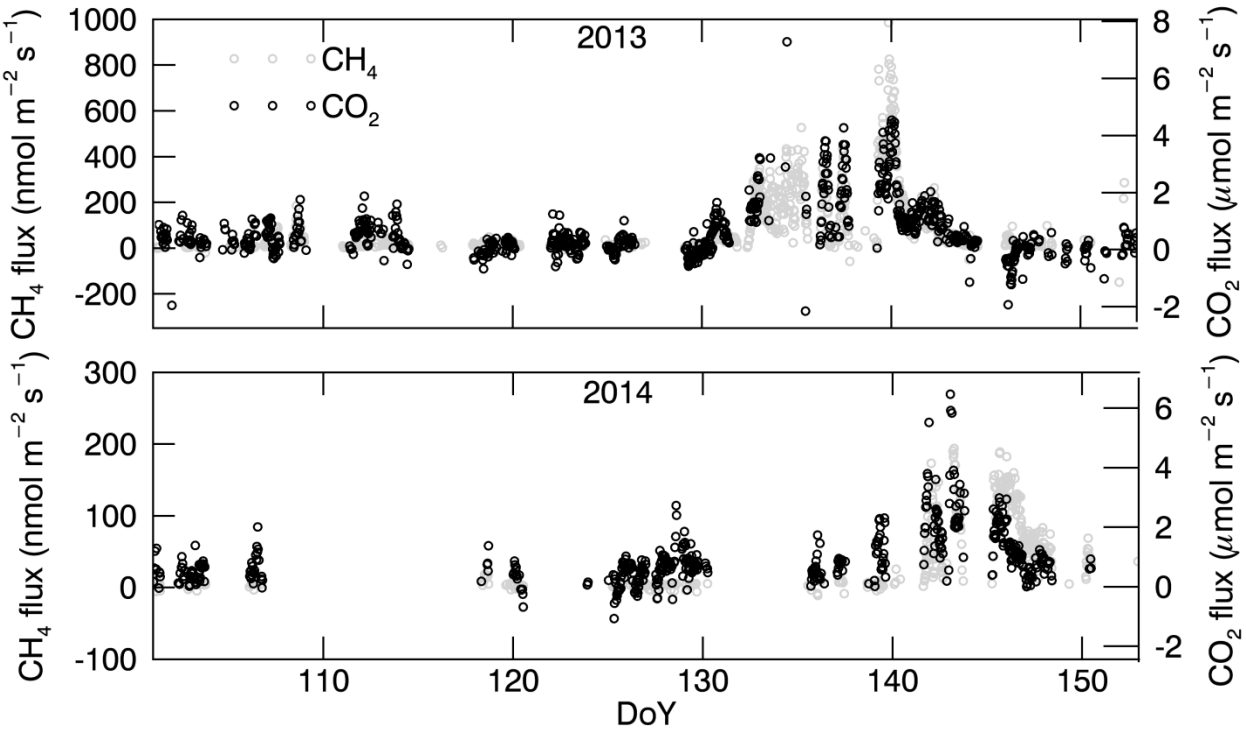

Figure S4. Measured CH_4 (grey) and CO_2 (black) half-hourly fluxes at the lake during the spring period of 2013 (top panel) and 2014 (bottom panel). The x-axis shows day of year. Note the difference in the scale of the y-axis between the two panels.

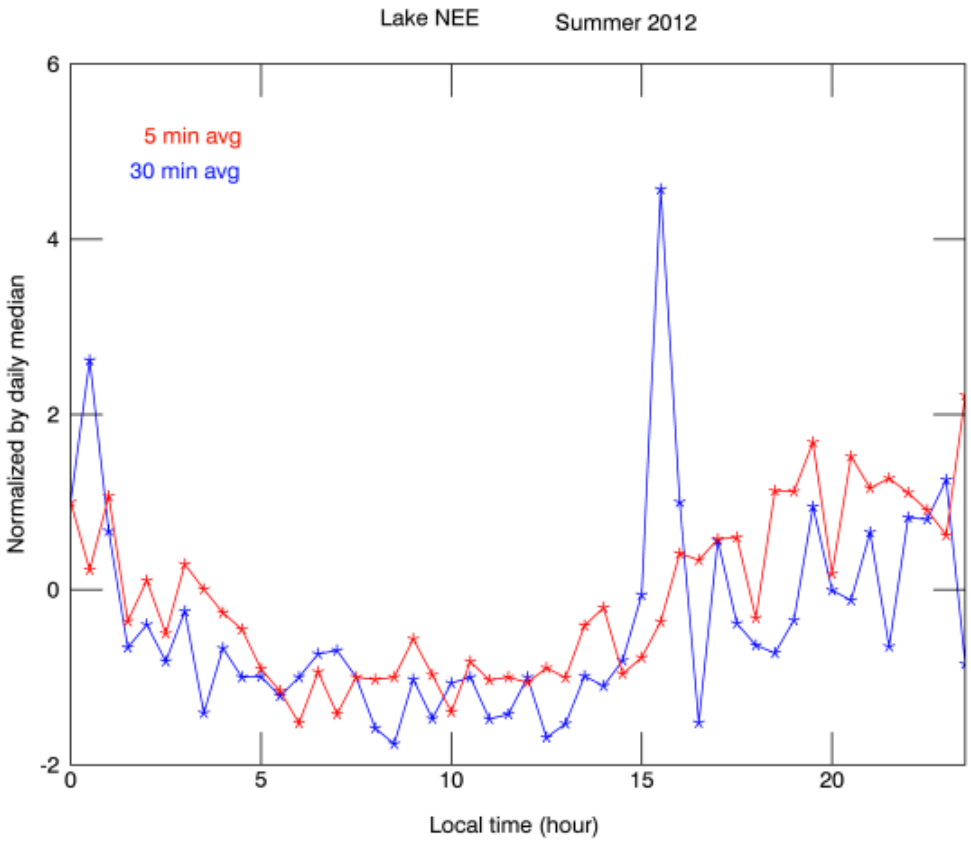

Figure S5. Diel course of the net CO_2 exchange at the lake surface, measured as 30 minutes averages (blue) and 5 minutes averages (red) in June-August 2012. Each dot represents a half-hour flux normalized by the daily median, i.e. the figure shows the deviation of each flux value from the daily median.

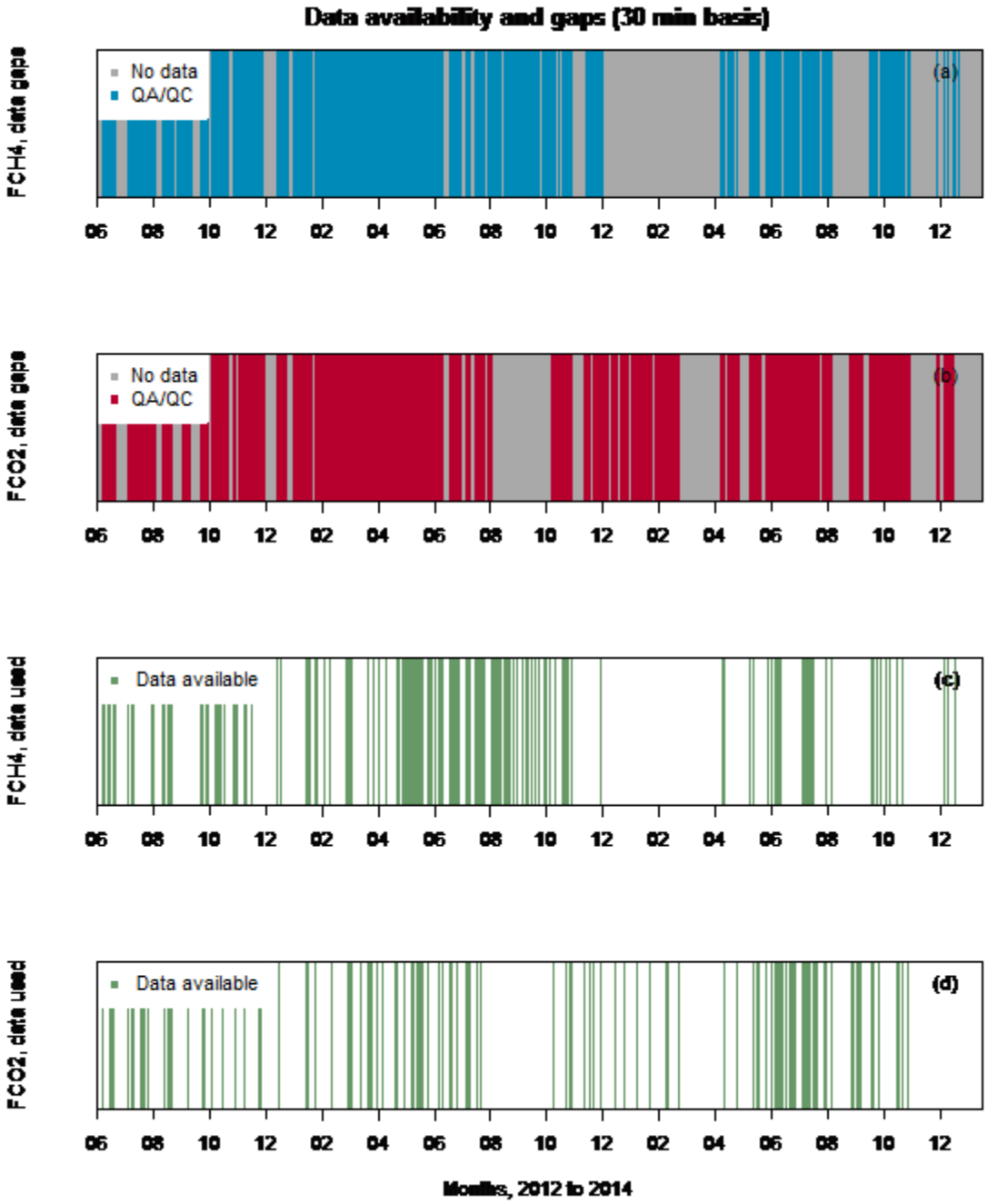

Figure S6. Visualization over the study period of data gaps due to filtering procedures (QA/QC), in the CH_4 (a) and CO_2 (b) flux time series, as well as the final dataset used in the study, CH_4 fluxes (c) and CO_2 fluxes (d). Grey periods in the two upper plots indicate the absence of data. During winter, measurements from the sonic anemometer and FGGA analyzer were regularly subject to multiple drop-outs and out-of-range values (filtered out during QA/QC), most likely due to frost on the sonic and very cold air input to the analyzer, which does not perform well at low temperature.